Journal of Loss Prevention in the Process Industries 71 (2021) 104495

Contents lists available at ScienceDirect

Journal of Loss Prevention in the Process Industries

journal homepage: http://www.elsevier.com/locate/jlp

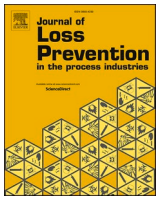

Evaluation of CFD simulations of transient pool fire burning rates

James R. Stewart [a,b,*], Herodotos N. Phylaktou [b], Gordon E. Andrews [b], Alan D. Burns [b]

[a] Health and Safety Executive (HSE), Harpur Hill, Buxton, SK17 9JN, UK
[b] School of Chemical and Process Engineering, University of Leeds, Leeds, LS2 9JT, UK

ARTICLE INFO

Keywords:
Fire modelling
Pool fire
Transient burning rate
CFD
Evaluation
FDS

ABSTRACT

Fire is the most commonly occurring major accident hazard in the chemical and process industries, with industry accident statistics highlighting the liquid pool fire as the most frequent fire event. Modelling of such phenomena feeds heavily into industry risk assessment and consequence analyses. Traditional simple empirical equations cannot account for the full range of factors influencing pool fire behaviour or increasingly complex plant design. The use of Computational Fluid Dynamics (CFD) modelling enables a greater understanding of pool fire behaviour to be gained numerically and provides the capability to deal with complex scenarios.

This paper presents an evaluation of the Fire Dynamics Simulator (FDS) for predictive modelling of liquid pool fire burning rates. Specifically, the work examines the ability of the model to predict temporal variations in the burning rate of open atmosphere pool fires. Fires ranging from 0.4 to 4 m in diameter, involving ethanol and a range of liquid hydrocarbons as fuels, are considered and comparisons of predicted fuel mass loss rates are compared to experimental measurements.

The results show that the liquid pyrolysis sub-model in FDS gives consistent model performance for fully predictive modelling of liquid pool fire burning rates, particularly during quasi-steady burning. However, the model falls short of predicting the subtleties associated with each phase of the transient burning process, failing to reliably predict fuel mass loss rates during fire growth and extinction. The results suggest a range of model modifications which could lead to improved prediction of the transient fire growth and extinction phases of burning for liquid pool fires, specifically, investigation of: ignition modelling techniques for high boiling temperature liquid fuels; a combustion regime combining both infinite and finite-rate chemistry; a solution method which accounts for two- or three-dimensional heat conduction effects in the liquid-phase; alternative surrogate fuel compositions for multi-component hydrocarbon fuels; and modification of the solution procedure used at the liquid-gas interface during fire extinction.

1. Introduction

Liquid pool fires are the most frequent type of fire event occurring in the process industries (Vasanth et al., 2013) with their prevalence due, in part, to the variety of circumstances in which they can occur. As well as standalone events, liquid pool fires are commonly involved in chains of ignition events collectively known as domino-effect accidents (Darbra et al., 2010; Abdolhamidzadeh et al., 2011; Vipin et al., 2018). The financial losses associated with large-scale industrial fires can be substantial, for example, four of the five largest process industry losses recorded in the year 2016–17 involved fire events responsible for property losses in excess of $1700 million (U.S) (Marsh, 2018). A vapour cloud explosion at the Indian Oil Corporation (IOC) terminal in Jaipur in 2009 (MoPNG Committee, 2010) led to the onset of multiple large-scale pool fires. The events led to the death of 12 people and injuries to 200 more as well as loss of the entire fuel inventory on site over a two week period of burning. This illustrates that such incidents can lead to considerable human harm and extensive damage to plant and the environment (Vipin et al., 2018). Industry accident statistics illustrate that around 60% of petrochemical storage tank accidents involve fire (Chang and Lin, 2006) with around 15–20 tank fires occurring per year since the 1990's (Persson and Lönnermark, 2004). The Persson and Lönnermark (2004) data covers a wide variety of fire types ranging from small scale rim seal fires to full surface tank fires, which implies that the number of large-scale pool fires or tank fires occurring is lower than the incident statistics suggest. Nevertheless, the incident data highlights the pool fire as a demonstrable hazard in the petrochemical industry. Additionally, reviews of worldwide domino-effect accident data indicate that fire is the primary event in around 40–55% of cases and that of

* Corresponding author. Health and Safety Executive (HSE), Harpur Hill, Buxton, SK17 9JN, UK.
E-mail address: james.stewart@hse.gov.uk (J.R. Stewart).

https://doi.org/10.1016/j.jlp.2021.104495
Received 11 September 2020; Received in revised form 9 March 2021; Accepted 6 April 2021
Available online 19 April 2021

Nomenclature

c_p	Specific heat capacity (kJ·kg^{-1}·K^{-1})
δx	Grid spacing (m)
ΔH_g	Heat of gasification (kJ·kg^{-1})
D	Pool diameter (m)
D^*	Characteristic fire diameter (m)
g	Acceleration due to gravity (m·s^{-2})
$k\beta$	Fuel-specific constant (m^{-1})
$\dot{m}''$	Mass loss flux (rate per unit area) (kg·s^{-1}·m^{-2})
$\dot{m}''_\infty$	Maximum mass loss flux (kg·s^{-1}·m^{-2})
$\dot{q}''_{fs}$	Incident heat flux on fuel surface (kW·m^{-2})
$\dot{Q}$	Heat release rate (kW)
T_∞	Ambient temperature (K)
Y_s	Soot yield (kg·kg^{-1})

those events initiated by fire, 80% began with pool fire incidents (Darbra et al., 2010; Abdolhamidzadeh et al., 2011). These findings clearly highlight the importance of the pool fire scenario when assessing fire risks for petrochemical sites.

Prevention and mitigation are the principal means of reducing the impact and likelihood of pool fire incidents. A key element of designing effective mitigation is a comprehensive understanding of pool fire burning behaviour, in which fire modelling plays an important role. Early modelling techniques used to estimate pool fire hazard quantities were generally based on correlations derived from well-defined sets of experiments. One of the more commonly-used approaches is that of Babrauskas (1983), which enables the pool fire steady-state fuel mass loss flux, $\dot{m}''$ (kg·s^{-1}·m^{-2}), to be estimated from a function of the maximum mass loss flux, $\dot{m}''_\infty$ (kg·s^{-1}·m^{-2}), the pool diameter, D (m), and a fuel-specific constant, $k\beta$ (m^{-1}), as described by Equation (1).

$$\dot{m}'' = \dot{m}''_\infty \left(1 - e^{-k\beta D}\right) \tag{1}$$

Later attempts moved towards the use of global energy balance approaches. These methods used a conservation of energy approach to estimate fuel vaporisation rates based on the extent of heat feedback to the fuel surface (de Ris and Orloff, 1972; Prasad et al., 1999; Hamins et al., 1999). More recently, correlations have been developed to account for the sootiness of the fuel (Ditch et al., 2013), which can have a significant impact on the heat flux incident to the fuel surface. The Ditch et al. (2013) approach is based on estimating the incident heat flux at the fuel surface, $\dot{q}''_{fs}$ (kW·m^{-2}), as a function of the fuel soot yield, Y_s (kg·kg^{-1}), heat of gasification of the liquid fuel, ΔH_g (kJ·kg^{-1}), and the pool diameter, D (m), as described by Equation (2). Equation (3) is then used to determine the quasi-steady fuel mass loss flux (Ditch et al., 2013).

$$\dot{q}''_{fs} = 12.5 + 68.3 {Y_s}^{1/4} \left[1 - e^{-\left(\frac{4}{3}\Delta H_g D\right)^{3/2}}\right] \tag{2}$$

$$\dot{m}'' = \frac{\dot{q}''_{fs}}{\Delta H_g} \tag{3}$$

Some relevant data for the input parameters required in Equations (1)–(3) are summarised in Table 1 and Table 2.

Pool fires are typically investigated in simple geometries as free spillages using either rectangular or circular trays to define the area of the pool. The liquid fuel depths used are usually shallow and less than 50 mm. However, process industry incidents often involve more complex scenarios, such as those with: process equipment in or near the fuel spillage area; pool fires resulting from process equipment leaks inside industrial plant with restricted air supply and ceiling accumulation of fire products (Chamberlain, 1996; Aljumaiah et al., 2014); pool fires located against vertical walls of storage vessels; pool fires inside deep fuel storage tanks. Whilst modelling approaches such as those of Babrauskas (1983) and Ditch et al. (2013) are useful, typically only requiring knowledge of the fuel properties and size of the pool, they are limited to predicting quasi-steady burning rates, rather than the transient burning rate profiles observed in fire tests (Pretrel et al., 2005). Furthermore, they cannot account for the complexities associated with process industry incidents. Computational Fluid Dynamics (CFD) modelling, on the other hand, enables a greater range of pool fire physics to be accounted for in the model. These models are more readily able to handle the complexities associated with real fire events and they are based on the solution of fluid flow governing equations. As such, they

Table 1
Summary of fuel properties used for the combustion and liquid evaporation models in FDS.

Parameter	Units	Ethanol[1,2]	Heptane [1-4]	TPH [5-8]	Diesel[9]	Gasoline[9]
Combustion Reaction						
Chemical formula	–	C_2H_6O	C_7H_{16}	$C_{12}H_{26}$	$C_{12}H_{26}$	C_8H_{18}
Soot yield	kg·kg^{-1}	0.008	0.037	0.015	0.015	0.038
Carbon monoxide yield	kg·kg^{-1}	0.001	0.010	0.006	0.006	0.011
Heat of combustion	MJ·kg^{-1}	25.6	41.3	42.0	42.0	44.5
Radiative fraction	–	0.25	0.33	0.35	0.35	0.31
Liquid Evaporation						
Boiling temperature	° C	78.35	98.35	188	216	68
Heat of vaporisation	kJ·kg^{-1}	837	317	361	280	317
Heat of gasification	kJ·kg^{-1}	913	439	751	737	388
Specific heat capacity	kJ·kg^{-1}·K^{-1}	2.44	2.24	2.40	2.40	2.06
Thermal conductivity	W·m^{-1}·K^{-1}	0.17	0.14	0.18	0.18	0.11
Absorption coefficient	m^{-1}	1140	333	300	300	200
Emissivity	–	1.0	1.0	1.0	0.95	0.95
Density	kg·m^{-3}	794	675	754	749	750

[1] McGrattan et al. (2019a,b).
[2] SFPE (2002).
[3] Hayasaka (1997).
[4] Yao et al. (2013).
[5] Le Saux et al. (2008).
[6] Audouin et al. (2011).
[7] van Hees et al. (2014).
[8] Stewart and Kelsey (2017).
[9] Rengel et al. (2018).

Table 2
Summary of the range of input parameter values used in the application of the Babrauskas (1983) and Ditch et al. (2013) correlations to estimated quasi-steady fuel mass burning rates.

Correlation & Input Parameters	Units	Ethanol	Heptane	TPH	Diesel	Gasoline
Babrauskas (1983)						
$\dot{m}''_\infty$	$kg{\cdot}s^{-1}{\cdot}m^{-2}$	0.022 [a]	0.101 [a]	0.048 [b]	0.048 [b] - 0.062 [c]	0.055[a] - 0.083 [c]
$k\beta$	m^{-1}	–	1.1 [a]	1.8 [b]	0.57 [d]–1.8 [b]	1.13 [c] - 2.1 [a]
Ditch et al. (2013)						
Y_s	$kg{\cdot}kg^{-1}$[a]	0.008 [a]	0.037 [a]	0.015 [e]	0.015[e]	0.038 [a]
ΔH_g [f]	$kJ{\cdot}kg^{-1}$[a]	913	439	751	737	388

[a] SFPE (2002).
[b] Pretrel (2006).
[c] Muñoz et al. (2004).
[d] Chatris et al. (2001a,b).
[e] Sikanen and Hostikka (2017).
[f] Estimated from data in Table 1 and SFPE (2002)

are not limited to a subset of scenarios on which the model is based, as is the case for simpler, empirical correlation approaches.

For the reasons outlined above, CFD modelling is regularly used in fire risk assessment, plant layout design and consequence analyses. For such applications significant assumptions are often made about the fire source with fuel mass loss rates imposed as boundary conditions in the models. Numerical modelling studies of this type have typically focussed on assessing other aspects of the models, such as the performance of heat, ventilation and air conditioning (HVAC) sub-models (Wahlqvist and van Hees, 2013; Beji et al., 2013, 2014), the choice of gas-phase combustion model (Wen et al., 2007; Stewart and Kelsey, 2017), or the turbulence closure model used in combination with the hydrodynamic solver (Vasanth et al., 2013). Where studies have considered the capability of models to predict fuel vaporisation rates for pool fires, the work has often been limited to fuel mass loss rates during the quasi-steady burning regime (Hostikka et al., 2002; Rengel et al., 2018). A number of authors have presented comparison of transient burning rate predictions to measured data (Suard et al., 2013; Wahlqvist and van Hees, 2016; Sikanen and Hostikka, 2016, 2017). However, these studies were primarily aimed at assessing fire model performance for simulating pool fires inside compartments, in which complex interactions between compartment conditions and fuel vaporisation rates exist. It is clear from the available literature that studies addressing model performance for simulating transient elements of open atmosphere pool fires is very limited.

The present study seeks to expand on the work of Rengel et al. (2018) by evaluating the ability of the Fire Dynamics Simulator (FDS) v6.7.0 to predict temporal variations in liquid pool fire fuel mass loss rates. The scenarios considered involve open atmosphere fires with ethanol and a variety of liquid hydrocarbons as fuels. The intention of the present study is to gain greater insight into where specific shortcomings of the current modelling approaches exist for predicting transient effects of liquid pool fire burning. The work has been undertaken with a view to assessing the implication of any areas of model weakness with regards to the practical application of CFD modelling of pool fires for industry risk assessment and consequence analyses. One of the key aims of the study is to use this work as a first step towards refining the modelling approach to enable reliable predictive simulations of liquid pool fire burning rates to be performed.

2. Methodology

The methodology used for the present study is based on direct comparison of model predictions to experimental data. FDS is used to predict transient burning rates for a number of pool fire scenarios involving a range of different liquid fuels and pool dimensions. Suitable experimental data is identified and compared to model predictions to evaluate the ability of the model to replicate observed transient features of pool fire burning. The performance of the model is evaluated both qualitatively and quantitatively through comparison to measured data and the application of statistical analysis techniques.

This Section outlines the criteria used to select appropriate experiments for model evaluation, gives an overview of the pool fire tests used, summarises the modelling approach adopted in the study and describes the process and metrics used to evaluate and critique model performance.

2.1. Selection of suitable experimental data

2.1.1. Criteria for selection

For the present study, CFD simulations are set up to reproduce liquid pool fire tests from a number of different experimental studies. The scenarios have been collectively chosen for use in the present modelling exercise since they represent well defined tests, span a range of fire sizes, involve a variety of liquid fuels and have transient pool fire burning rate, heat release rate (HRR) or regression rate measurements available in the original research papers. Each experiment considered was either an open atmosphere test or involved a fire contained within a sufficiently large enclosure to give conditions representative of an open atmosphere.

2.1.2. Selected experimental data

Pool sizes ranging from around 0.4 m to 4 m in diameter with estimated heat release rates ranging from roughly 0.1 MW to 31 MW have been simulated. For each test considered, the data presented in the original research has been digitally processed to produce a dataset suitable for comparison to FDS model predictions. A full description of each fire test used can be found from the relevant references, with only a brief outline provided below for context. The experiments considered are summarised in Table 3.

Hostikka et al. (2001) performed a series of fire tests inside medium

Table 3
Summary of the fire tests modelled.

Experimental Study	Fuel	Fire Area (m^2)	Fuel Depth (mm)	Modelled Pool Side Length (m)	Grid Spacing δx (cm)
Hostikka et al. (2001)	Heptane	1.07	25.0	1.03	6.1
		2.00	22.0	1.41	8.3
Chatris et al. (2001a, b)	Diesel	12.57	9.5	3.55	20.9
	Gasoline		9.0		
Muñoz et al. (2004)	Diesel	1.77	38.1	1.33	7.8
	Gasoline	7.07	41.4	2.66	15.6
Pretrel et al. (2005)	TPH	0.1	48.7	0.32	1.9
		0.2	51.1	0.45	2.8
		0.4	50.1	0.63	4.0
Thomas et al. (2007)	Ethanol	0.57	8.8	0.75	4.4

and large scale enclosures at the VTT Technical Research Centre of Finland. Data for two heptane pool fire tests from this experimental programme is used here. Both tests were undertaken inside a 27 m x 14 m x 19 m burn hall, which was sufficiently well-ventilated to approximate an open atmosphere. The two pool fires were circular with areas of 1.07 m^2 and 2.0 m^2. The available measured data has been averaged across a number of repeat fire tests (Hostikka et al., 2001; McGrattan et al., 2019a).

A comprehensive series of outdoor pool fire tests using gasoline and diesel as fuels with pool diameters of 1.5 m, 3 m and 4 m was undertaken by Chatris et al. (2001a, b). Transient mass burning rate data for two of the 4 m diameter fires is available, one with diesel, the other gasoline, as the fuel. Muñoz et al. (2004) performed a further series of tests using the same experimental facility as an extension of the Chatris et al. (2001a, b) work. These tests included fires with 5 m and 6 m diameters. Transient burning rate data is presented by Muñoz et al. (2004) for a 1.5 m diameter diesel pool fire and a 3 m diameter gasoline pool fire. Data from these four fire experiments is used for comparison to FDS model predictions in the present work.

The PRISME (*Propagation d'un Incendie pour des Scénarios Multilocaux Elémentaires*) project, coordinated by the OECD Nuclear Energy Agency (NEA), is a joint international research project focussing on fires in nuclear power plants. Data from a selection of the support tests conducted as part of the PRISME Source campaign is used here. The PRISME Source tests were undertaken to characterise the burning behaviour of pools of hydrogenated tetra-propylene (TPH), a fuel used in nuclear fuel reprocessing, under a large-scale cone calorimeter. The tests, described by Pretrel et al. (2005), involved fires in 10 cm deep circular pans with areas of 0.1, 0.2 and 0.4 m^2 and an initial fuel depth of approximately 5 cm. FDS predictions of fuel burning rates for three of these tests, one for each pool size, are compared to the experimental fuel mass loss rate data.[1] Numerous authors, including Suard et al. (2011, 2013), Wahlqvist and van Hees (2013, 2016), Beji et al. (2013, 2014), van Hees et al. (2014), Sikanen and Hostikka (2017), Stewart and Kelsey (2017), have used data from the PRISME or PRISME-2 experiments for the purposes of model evaluation.

Thomas et al. (2007) performed open atmosphere and compartment fire tests using one or more steel fuel trays 0.81 m x 0.70 m x 0.05 m in size each containing 5 l, 10 l or 20 l of methylated spirit (97% ethanol, 3% water). The experiments were undertaken to produce data for the validation of liquid pool fire models. Transient heat release rate data for a 5 l single tray test in the open atmosphere will be used for that purpose in this work. The authors compared model predictions made using FDS v4 to their measurements. The same test was considered in an exercise to evaluate an earlier version of FDS v6 by Zadeh et al. (2015, 2016).

2.2. Numerical modelling

2.2.1. Description of the CFD model

The Fire Dynamics Simulator (FDS) v6.7.0 (McGrattan et al., 2019a, b) was used to perform the simulations described in this paper. FDS is a Large Eddy Simulation (LES) CFD model that solves a discretised form of the Navier-Stokes equations appropriate for modelling low-Mach number, thermally-driven fluid flows. The LES formulation uses the Deardorff eddy viscosity model for sub-grid-scale closure with constant turbulent Schmidt and Prandtl numbers. The governing equations of fluid flow are discretised using central finite differences on a structured, Cartesian mesh with staggered grid storage. The solution procedure is based on an explicit, second-order Runge-Kutta numerical scheme. Gas-phase combustion is treated using a single-step, infinitely-fast mixing-controlled reaction of three lumped species, namely, fuel, air and products of combustion. To account for the effects of thermal radiation in the gas phase, FDS uses the Finite Volume Method (FVM) to solve the Radiative Transport Equation (RTE) for a gray-gas (McGrattan et al., 2019a, b).

In the present study, the fire boundary condition is described using a liquid evaporation model. In this model, the rate of fuel evaporation is dependent on the fuel temperature and the concentration of fuel vapour above the liquid surface. The evaporation rate is governed by Stefan diffusion, which determines the mass of fuel vaporised based on an empirically derived mass transfer coefficient for the fuel surface (McGrattan et al., 2019a). The liquid fuel is treated as a thermally-thick solid for the purposes of heat conduction. Convection inside the liquid fuel layer is not accounted for by the model. As a consequence, the convection currents present in the liquid phase will not be captured by the model, which will affect the extent of liquid phase heat transfer. However, convective heat transfer at the liquid-gas interface is modelled in the gas phase solution. For the majority of the fire experiments considered in this work, the pool size is such that the fire is in the optically-thick, radiative burning regime (Babrauskas, 1983), thus the influence of convective flows within the fuel layer is expected to be small. Full descriptions of the equations used can be found in McGrattan et al. (2019a) and are also given by Sikanen and Hostikka (2016, 2017).

For the simulations described here FDS has been used with its default sub-model settings, with the exception of the use of the liquid evaporation model, which whilst used in its standard form, is not the approach typically used to represent a fire in FDS. More commonly the fire heat release rate, or the fuel mass loss rate, is imposed as the fire boundary condition in an FDS simulation. The purpose of using FDS in the manner described here is to determine how the existing sub-models perform when applied to the prediction of transient mass burning rates for liquid pool fires.

2.2.2. Boundary conditions

The material properties for the fuel pan, any insulating materials and, for the case of outdoor tests, the concrete substrate on which the tests were performed have been specified using the data given in Table 4. The fuel properties used for the combustion reaction and liquid evaporation model are given in Table 1.

The choice of fuel properties introduces significant uncertainty for the modelling of multi-component fuels such as diesel and gasoline. These fuels contain multiple hydrocarbon components having a range of boiling points, for example, around 25 °C to 210 °C for petrol (gasoline) and between 160 °C to 360 °C for diesel (del Coro Fernández-Feal et al., 2017). Treating these fuels as fixed boiling point liquids could lead to significant prediction error. The use of 68 °C as the boiling point for gasoline in the modelling presented here neglects the very high rate of production of volatiles at lower temperatures. Conversely, the use of 216 °C as the boiling point of diesel is at the low end of the anticipated range of boiling points for a diesel mixture, thus giving a more readily evaporating fuel in the model than should be the case. Similar issues are expected to arise as a result of using single values for the fuel heats of vaporisation when gasoline and diesel are multi-component mixtures

Table 4
Summary of material properties used in the FDS simulations.

Parameter	Units	Steel [a]	Water [a]	Concrete [b]	Rock Wool Insulation [b]
Density	$kg \cdot m^{-3}$	7850	1000	2430	140
Specific heat capacity	$kJ \cdot kg^{-1}{}^{a} \cdot K^{-1}{}^{a}$	0.46	4.20	0.74	0.84
Thermal conductivity	$W \cdot m^{-1}{}^{a} \cdot K^{-1}{}^{a}$	45.8	0.53	1.50	0.10
Emissivity	–	1.0	1.0	0.70	0.95

[a] https://github.com/firemodels/fds/blob/master/Validation/Pool_Fires/FDS_Input_Files/VTT_heptane_1_m2.fds accessed 5th June 2020.
[b] Audouin et al. (2011).

[1] Data from the PRISME project is freely available and can be requested from the Nuclear Energy Association data bank here: http://www.oecd-nea.org/tools/abstract/detail/csni2006/.

having a range of values. The boiling temperatures used here are taken from the work of Rengel et al. (2018) and have been used to ensure consistency across the two studies. However, it is expected that the burning rates for the gasoline and diesel fires modelled here will be under and over predicted, respectively.

The majority of the experiments used to provide burning rate data for the present study were undertaken in the absence of wind, with the exception of the two Chatris et al. (2001) tests and one of the Muñoz et al. (2004) tests, in which a light wind was blowing across the pool. Chatris et al. (2001) noted that the influence of wind was negligible for wind speeds below 2 m·s^{-1}, which is the case for all of the tests considered, thus the effect of wind was not included in the model. Instead the domain boundaries in the FDS model were specified as 'open' boundaries, with the exception of the boundary representing the ground, which was modelled using the 'inert' boundary type in FDS.

As such, the fuel boiling point specified as a model input is of critical importance and the use of a single boiling point as an approximation for multi-component fuels, such as diesel and gasoline, can lead to significant prediction errors for such fuels.

In all cases the fire source is modelled using a square cross-section to align with the structured Cartesian mesh used in FDS. The dimensions of the modelled fire source were such that the fuel surface area in the model remained consistent with that of the corresponding experiment. The use of a square fire source introduces an element of uncertainty with regards to air entrainment into the fire plume, since a square fuel pan will have a proportionately larger perimeter than a circular pan of equivalent area. However, since the present study is focussed primarily on fuel mass loss fluxes, maintaining the correct fuel surface area is considered to be a more important element of capturing the pool fire source in the model. Another important factor associated with matching the fire source area in the model to that used in the experiments is that this enables the correct fuel depth to be imposed in the model for the given volume of fuel used in each experiment simulated. As a result, the fire area, fuel depth and fuel quantity used in the model correspond to the quantities used in the experiments. For scenarios in which the sides of the fuel pan extend above the liquid surface, this unwetted part of the pan wall was also incorporated in to the model and the grid resolution was specified such that it was sufficient to capture the lip with at least one grid cell.

2.2.3. Mesh resolution and computational domain

The computational meshes used in this work comprise Cartesian grid cells with dimensions based on the characteristic fire diameter, D^*, given by Equation (4) (McGrattan et al., 2019b). Here $\dot{Q}$ (kW) is the fire heat release rate and ρ_∞ (kg·m^{-3}), c_p (kJ·kg^{-1}·K^{-1}) and T_∞ (K) are the ambient density, specific heat capacity and temperature, respectively.

$$D^* = \left(\frac{\dot{Q}}{\rho_\infty c_p T_\infty \sqrt{g}} \right)^{2/5} \tag{4}$$

Model sensitivity to the choice of numerical grid resolution was assessed using a range of meshes with grid spacing, δx, such that $5 \leq (D^*/\delta x) \leq 25$. The selected range of cell sizes give a slightly improved resolution of the fire source compared to those used in the validation of FDS undertaken by the U.S. Nuclear Regulatory Commission (2007). Total cell counts between 17,640 and 2,040,200 were used across the range of simulations undertaken. The grid sensitivity analysis results demonstrated that the coarsest mesh used often gave very different results to those obtained using other grid resolutions. This is likely as a result of there being insufficient resolution to capture the fuel pan lip, which is known to strongly affect fuel burning rates (Zadeh et al., 2015; 2016). The differences in predictions across the other meshes were smaller. An example of the grid sensitivity analysis results is shown in Fig. 1 for predictions of the burning rate for the Thomas et al. (2007) 0.57 m^2 ethanol pool fire test. This Figure demonstrates that using a lower grid resolution gives, in this case, a shorter fire duration, lower quasi-steady burning rate and premature period of burning rate decay than the two higher resolution computational meshes.

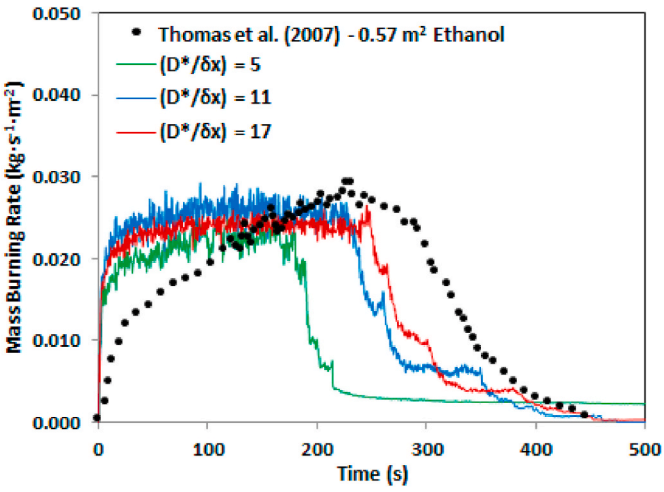

Fig. 1. Grid sensitivity analysis results showing a comparison of measured and predicted mass burning rates per unit area for the Thomas et al. (2007) 0.57 m^2 ethanol pool fire.

Error bars are included in comparisons between model predictions and experimental data presented in Section 4 to illustrate the level of mesh sensitivity for predictions of quasi-steady burning rates across the range of fire tests modelled. The main results presented in this paper were produced using mesh resolutions having $D^*/\delta x = 17$, comparable to the fine mesh resolution used in previous validation of FDS, where $D^*/\delta x = 16$ (U.S. Nuclear Regulatory Commission, 2007). The specific grid spacing used for each case is given in Table 3.

The computational domain was specified so as to ensure that fuel combustion takes place entirely within the simulated domain. As a result, domain sizes approximately 4 x 4 x 8 times the fire diameter were used for all cases considered.

2.2.4. Modelling fuels and fuel ignition

For the cases involving heptane and ethanol as fuels, default fuel species from the FDS material library were used. Where the fuel was gasoline the FDS species *n*-Octane was used as a surrogate fuel. For the diesel and TPH pool fire cases, dodecane was specified as the surrogate fuel in the model. To ensure that the model captures the desired fuel properties, the FDS defaults were modified as shown by the values given in Table 1. The multi-component fuels considered, e.g. diesel and gasoline, would typically contain a range of hydrocarbons of varying carbon chain lengths and boiling temperatures. The use of a single component surrogate fuel with a single boiling point in the model is a broad approximation of the reality. However, such simplifications are common for process safety risk and consequence analyses, thus the use of such an approach in the present work is considered to give a modelling approach which is representative of that used in industrial applications. Implications of this modelling approach for prediction of transient mass burning rates are discussed, particularly for gasoline, in Section 3.1.

For the simulations with diesel or TPH as the fuel, it was necessary to model ignition explicitly due to the relatively high boiling temperatures imposed for the fuels (see Table 1). The method used involved defining a solid obstruction with a fixed surface temperature of 1000 °C just above the fuel surface for the first 30 s of each simulation. Heat transfer from this 'hot block' to the fuel surface enables the fuel temperature to increase above its boiling point, leading to fuel vaporisation and subsequent combustion in the model. This approach is similar to that used in the work of Sikanen and Hostikka (2017) and Rengel et al. (2018). A 10 kW propane burner was used as the ignition mechanism for the Pretrel

et al. (2005) tests with the flame seen to spread from the ignition location to cover the entire pool surface shortly after the start of each test. The ignition mechanism used for the other experiments modelled here is not explicitly described in the original work, thus no further details can be provided here.

2.3. Evaluation

2.3.1. Fire parameters monitored

The evaluation of FDS performance presented here considers the ability of the model to qualitatively capture features of transient liquid pool fire burning behaviour by comparison of predicted and observed transient fuel mass burning rates. Quantitative comparison of model predictions to experimental measurements is also made through the application of statistical performance analysis techniques, as described in Section 2.3.3. FDS predictions of quasi-steady burning rates are also compared to estimates made using the empirical correlations introduced in Section 1.

For the quantitative analysis, estimates of the predicted fire growth, quasi-steady and extinction phase durations, the total burn duration, the time to the onset of the extinction phase, the quasi-steady burning rate, the maximum burning rate and the maximum 60 s time-averaged burning rate are compared to measurements. Relevant durations of each phase of the transient burning process were determined from 5 s rolling averages of the measured and predicted burning rates.

For the experiments, the observed quasi-steady burning rate and duration were used in the comparison, with the end of the growth phase taken to be the observed start of quasi-steady burning. The start of the extinction phase was taken to be the final time at which the 5 s averaged burning rate fell below the measured steady-state burning rate for each test.

For the model, the quasi-steady burning rate was taken to be the average predicted burning rate over the measured steady-state burning period. The end of the fire growth phase and the start of the extinction phase were taken to be the first and final times at which the 5 s averaged burning rate reached the predicted quasi-steady burning rate. The end of the extinction phase was taken to be the time at which the predicted burning rate fell below a threshold of 1 $g{\cdot}s^{-1}{\cdot}m^{-2}$, which represents between 1% and 4% of the measured quasi-steady burning rates across all tests modelled. This threshold value, whilst somewhat arbitrary, has been used to ensure that all of the predicted extinction phase is captured in the analysis.

Both the experimental data and the model predictions were processed to determine a maximum burning rate, which was taken to be the maximum of a 1 s rolling average burning rate to avoid spurious instantaneous peaks, particularly in the measured data. In addition, the transient burning rate measurements and predictions were processed to produce 60 s time-averaged burning rates with the maximum over this longer duration also compared.

2.3.2. Comparison to empirical correlations

In addition to the comparison of model predictions and experimental measurements, predicted quasi-steady burning rates are also compared to estimates made using the empirical correlations of Babrauskas (1983) and Ditch et al. (2013). The input parameter values used in these correlations are summarised in Table 2 for each fuel considered in the present study. Note that for ethanol, a constant burning rate per unit area of 0.022 $kg{\cdot}s^{-1}{\cdot}m^{-2}$ is prescribed for fire diameters ranging from 0.6 m to 3.0 m (SFPE, 2002), thus no value is given for the coefficient $k\beta$ for ethanol in Table 2.

2.4. Statistical performance analysis

Statistical analysis techniques have been used to compare the range of measured and predicted transient liquid pool fire properties outlined in Section 2.3.1. Specifically, two of the Statistical Performance Measures (SPM) commonly used in the evaluation of atmospheric dispersion models (Hanna et al., 1993; Chang and Hanna, 2004; Papanikolaou et al., 2010; Ivings et al., 2016) have been used, namely, the geometric mean bias (MG) and the geometric variance (VG), which enable quantitative assessment of model prediction bias and scatter, respectively.

The parameters MG and VG can be calculated from pairs of measured, M, and predicted, P, data using Equations (5) and (6). Here the angled brackets $\langle \ldots \rangle$ denote the average across all measured/predicted pairs of data. Values of $MG = 0.5$ and $MG = 2.0$ indicate a model which under- and over-predicts the mean by a factor of two, respectively. It should be noted that for MG and VG as described here, the predicted and measured variables are used the opposite way around to that used in the original methodology (Hanna et al., 1993). The reason for this is to give a more intuitive plot of MG versus VG such that values of MG greater than 1 represent over-prediction and values of MG less than 1 represent under-prediction.

$$MG = exp < \ln\left(\frac{P}{M}\right) > \tag{5}$$

$$VG = exp < \left[\ln\left(\frac{P}{M}\right)\right]^2 > \tag{6}$$

What constitutes a ‘good’ model in terms of MG and VG values is not easily defined. From their extensive analysis of atmospheric dispersion model evaluation studies, Chang and Hanna (2004) conclude that a ‘good’ model would be expected to achieve a mean bias within ±30% of the mean and a scatter of around 2 to 3 of the mean. In terms of the parameters MG and VG these suggested levels of model performance equate to roughly $0.7 < MG < 1.3$ and $VG < 3.3$. Similar criteria have been adopted in the work of Papanikolaou et al. (2010), though the authors suggest $VG < 4$. In the LNG MEP, Ivings et al. (2016) recommend slightly broader model acceptance criteria, using a mean bias within ±50% of the mean.

The concept of using statistical measures to evaluate model performance is firmly based in the study of atmospheric dispersion modelling, rather than the evaluation of fire models. The criteria outlined above to distinguish better performing models were developed strictly for the evaluation of dispersion model results in comparison to research grade field trials. Whether the same criteria can reasonably be used to categorise fire model performance is questionable and as such these criteria are included for reference only in the present work. In Section 4.4, MG and VG values are presented for the range of transient fire quantities discussed in Section 2.3.1 as a means of characterising the model performance using simple statistical measures. Further research to develop a set of quantitative acceptance criteria suitable for evaluating the performance of fire models is needed.

3. Results

3.1. Transient fuel mass burning rate

The results presented in this Section focus on the qualitative comparison of predicted and measured time-varying fuel mass burning rates across the burn duration as a whole. A number of other authors have compared FDS predictions of burning rates for liquid fuel pool fires to measured data but such studies have typically concentrated on the quasi-steady period of burning. The analysis presented in Section 4 considers the individual stages of fire development in order to provide insight into FDS performance through the transient burning process.

Fig. 2 to Fig. 5 compare the measured and predicted time-varying mass burning rate per unit area for each of the fire tests listed in Table 3. Each Figure shows the FDS predictions in red and the experimental data in black. Quasi-steady burning rates, estimated through the application of the Babrauskas (1983) and Ditch et al. (2013) correlations

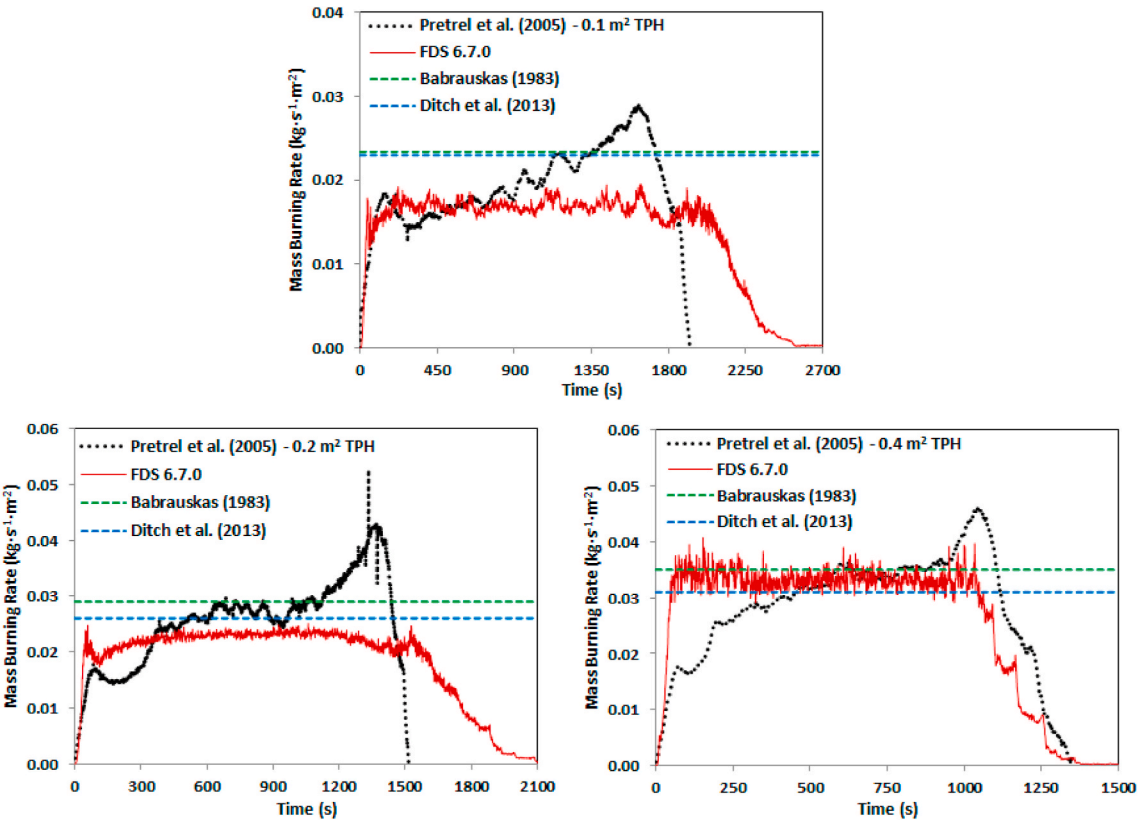

Fig. 2. Comparison of measured and predicted mass burning rates per unit area for the Pretrel et al. (2005) 0.1 m^2 (top), 0.2 m^2 (bottom-left) and 0.4 m^2 (bottom-right) TPH pool fires. Estimated steady-state burning rates calculated using the Babrauskas (1983) and Ditch et al. (2013) correlations are shown by the dashed green and blue lines, respectively. (For interpretation of the references to colour in this figure legend, the reader is referred to the Web version of this article.)

discussed in Section 1, are also shown in the Figures using dashed green and blue lines, respectively. For the scenarios involving diesel or gasoline as fuels, Chatris et al. (2001a, b) and Muñoz et al. (2004) give alternative values for the constants used in the Babrauskas (1983) correlation, as summarised in Table 2. For these cases, ranges of quasi-steady burning rates, estimated using the data from Table 2 and Equation (1), are shown as pale green bands across Fig. 3.

Comparing the model predictions across the range of tests simulated illustrates that FDS consistently predicts a three-phase burning rate profile, broadly comprising fire growth, quasi-steady burning and extinction. Generally the model gives reasonable agreement with the experimental data across the range of tests considered, but the different phases of the transient burning process are not captured correctly by the model. Qualitative agreement between FDS and the experiments is given for cases where the measured burning rate profile is relatively simple, for example the heptane pool fires of Hostikka et al. (2001) shown in Fig. 4. Where other physical mechanisms introduce more complex pool fire burning behaviours the predicted transient burning rate profile is less well-matched to the measurements, for example, for the boilover-induced peak in burning rate prior to extinction for the Muñoz et al. (2004) diesel test (Fig. 3), or the increase in burning rate prior to extinction for the TPH fires of Pretrel et al. (2005) (Fig. 2) as a result of increased conduction between the fuel pan and the shallow fuel layer during the final stages of the burn. Section 1 presents further analysis of the model results during each phase of burning and makes recommendations for possible model changes to address the disagreement between model predictions and the measured data.

Figs. 2 to 5 also show that there are large discrepancies between the quasi-steady burning rates estimated using the Babrauskas (1983) and the Ditch et al. (2013) correlations for the gasoline and heptane fires in particular. This demonstrates that there are significant uncertainties associated with the input parameters used in the correlations. The multi-component nature of gasoline means that it is difficult to provide generic model inputs for empirical correlations which cover the broad range of fuel compositions that could be encountered. Quantitative comparison of the measured burning rate to the two considered empirical correlations is given in Section 4.4.

4. Analysis and discussion

4.1. Rate of fire growth

The FDS modelling undertaken here is based on the use of an infinitely-fast, mixing-controlled, single-step combustion reaction. This enables combustion to occur in the model wherever fuel vapour and oxygen co-exist such that their reaction would generate sufficient heat to raise the local grid cell temperature above the critical flame temperature (CFT) of the fuel (McGrattan et al., 2019a). In the present modelling the FDS default CFT values were used for each fuel species, ranging from 1397 K to 1507 K, corresponding to the lean limit adiabatic flame temperatures for premixed hydrocarbon/air mixtures (SFPE, 2002). For the fuels having a relatively low boiling temperature, namely ethanol, heptane and gasoline, ignition is instantaneous in the model and the predicted rates of fire growth greatly exceed those observed in the corresponding experiments. Conversely, for diesel and TPH, whose boiling temperatures are higher, a source of ignition must be explicitly defined in the model. For the modelling involving such fuels the result is a slower predicted initial rate of fire growth which more closely agrees with the measured data.

Figs. 6 and 7 show the progression of the flame across the fuel surface for the 0.57 m^2 ethanol (Thomas et al., 2007) and the 0.4 m^2 TPH (Pretrel et al., 2005) pool fires, respectively, during the first 60 s of simulation. For the ethanol fire the flame covers the entire fuel surface immediately and the quasi-steady burning regime is reached quickly, as

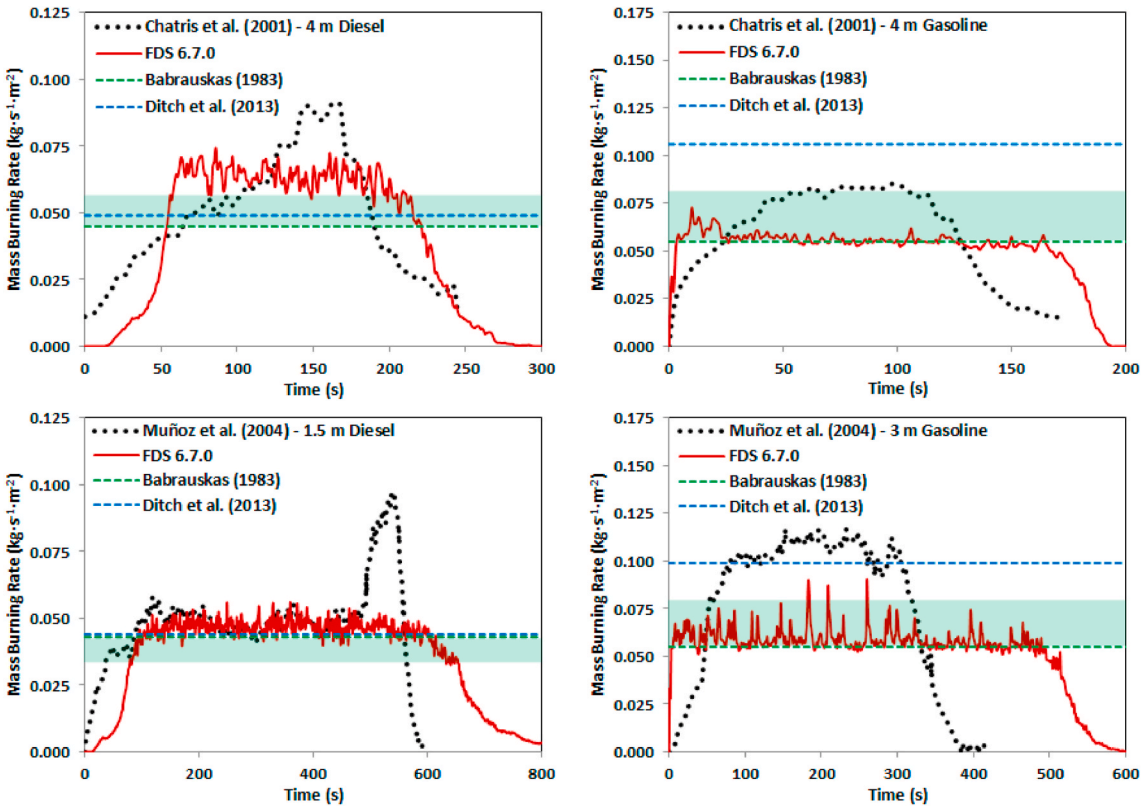

Fig. 3. Comparison of measured and predicted mass burning rates per unit area for the Chatris et al. (2001) 4 m diesel (top-left) and 4 m gasoline (top-right) and the Muñoz et al. (2004) 1.5 m diesel (bottom-left) and 3 m gasoline (bottom-right) pool fires. Estimated steady-state burning rates calculated using the Babrauskas (1983) and Ditch et al. (2013) correlations are shown by the dashed green and blue lines, respectively. The ranges of burning rates given by the Babrauskas (1983) correlation using the range of inputs shown in Table 2 are shown by the pale green bar in each part of the Figure. (For interpretation of the references to colour in this figure legend, the reader is referred to the Web version of this article.)

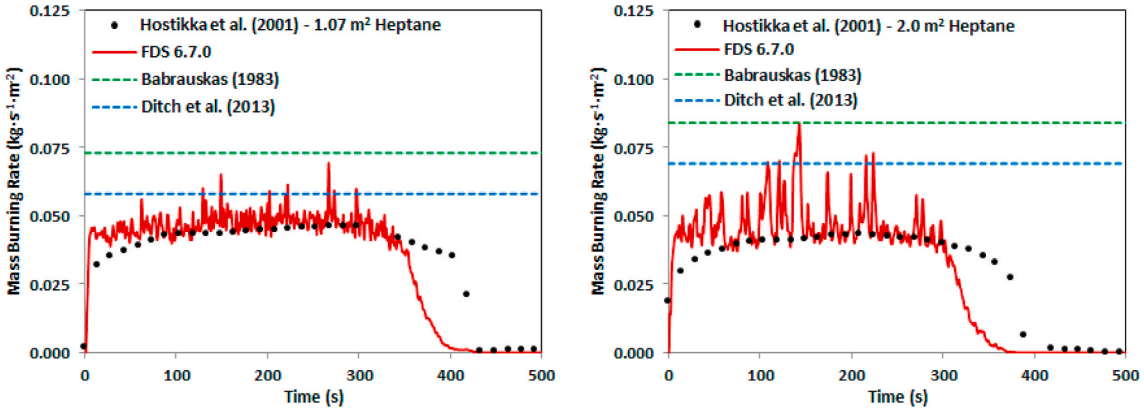

Fig. 4. Comparison of measured and predicted mass burning rates per unit area for the Hostikka et al. (2001) 1.07 m^2 (left) and 2.0 m^2 (right) heptane pool fires. Estimated steady-state burning rates calculated using the Babrauskas (1983) and Ditch et al. (2013) correlations are shown by the dashed green and blue lines, respectively. (For interpretation of the references to colour in this figure legend, the reader is referred to the Web version of this article.)

shown in Fig. 5, indicating that the model predicts rapid fire growth for this fuel. However, for the TPH fire it takes longer for the flame to spread across the fuel surface, indicating a slower initial rate of fire growth, which can be seen to more closely agree with the initial measured growth rate as shown in Fig. 2. For the TPH and diesel fires, once the flame covers the entire pool surface the rate of fire growth approximates that of the lower boiling temperature fuels, greatly exceeding the rates observed during the experiments. This behaviour is illustrated clearly in Fig. 2 for the 0.4 m^2 TPH pool fire of Pretrel et al. (2005), with the predicted initial rate of growth closely matched to the measurements before accelerating further to reach a quasi-steady state.

A 10 kW propane burner was used as the ignition mechanism for the Pretrel et al. (2005) TPH fire tests. Heat transferred from the burner to the liquid pool surface was confined to a small area in which the flame from the burner contacts the TPH fuel surface. As a result, the initial pool fire flame spreads from a small area, relative to the pool size, and the fire growth is gradual, as shown in Fig. 2. In the modelling, the hot block used to ignite the TPH pool resulted in heat transfer to a larger area of the pool than was the case for the burner used in the experiments. Consequently, the initial flame region for the TPH pool was larger in the

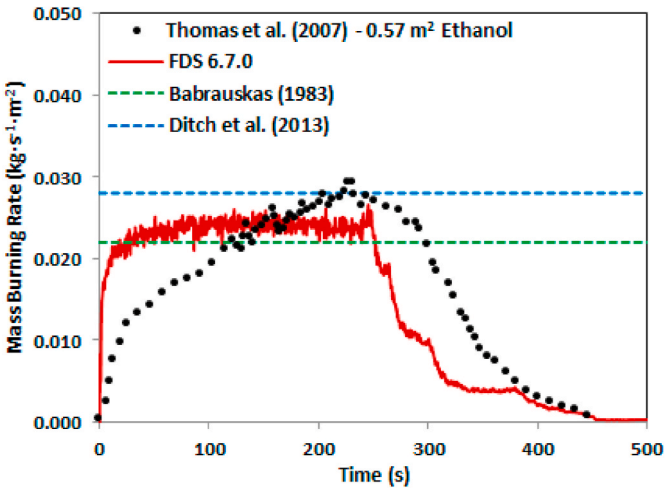

Fig. 5. Comparison of measured and predicted mass burning rates per unit area for the Thomas et al. (2007) 0.57 m^2 ethanol pool fire. Estimated steady-state burning rates calculated using the Babrauskas (1983) and Ditch et al. (2013) correlations are shown by the dashed green and blue lines, respectively. (For interpretation of the references to colour in this figure legend, the reader is referred to the Web version of this article.)

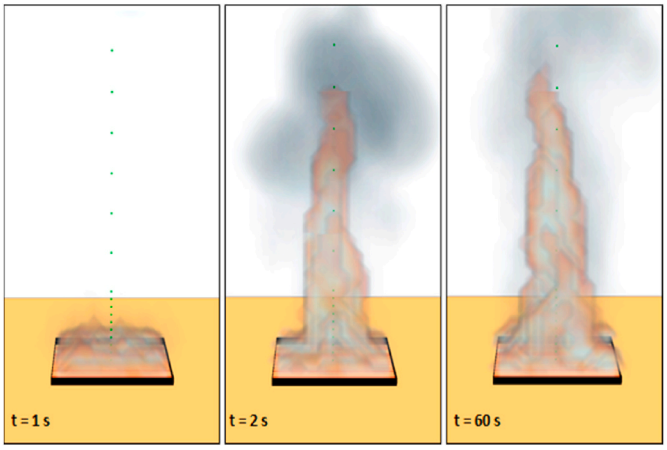

Fig. 6. FDS predicted fire growth for the Thomas et al. (2007) 0.57 m^2 ethanol pool fire.

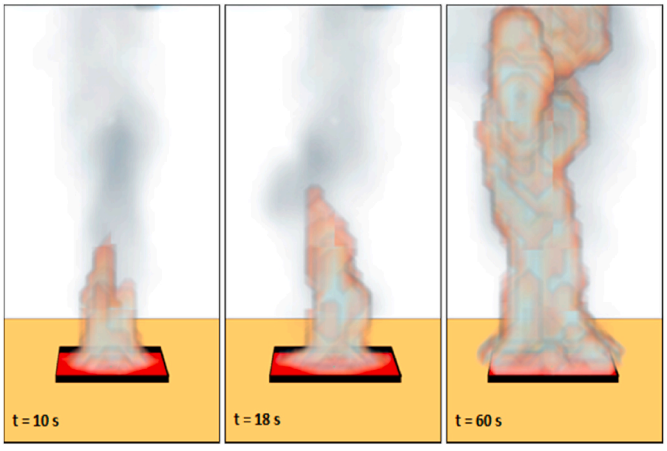

Fig. 7. FDS predicted fire growth for the Pretrel et al. (2005) 0.4 m^2 TPH pool fire.

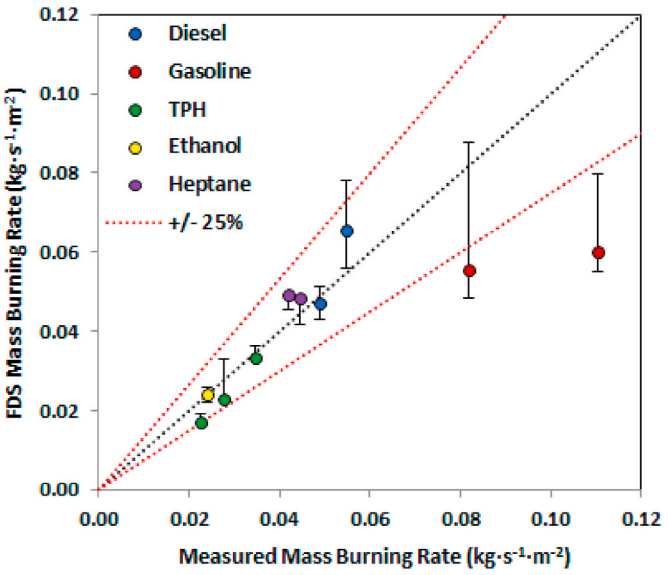

Fig. 8. Comparison of FDS-predicted and measured quasi-steady fuel mass burning rates for each fire test simulated with the FDS grid sensitivity results illustrated using vertical error bars.

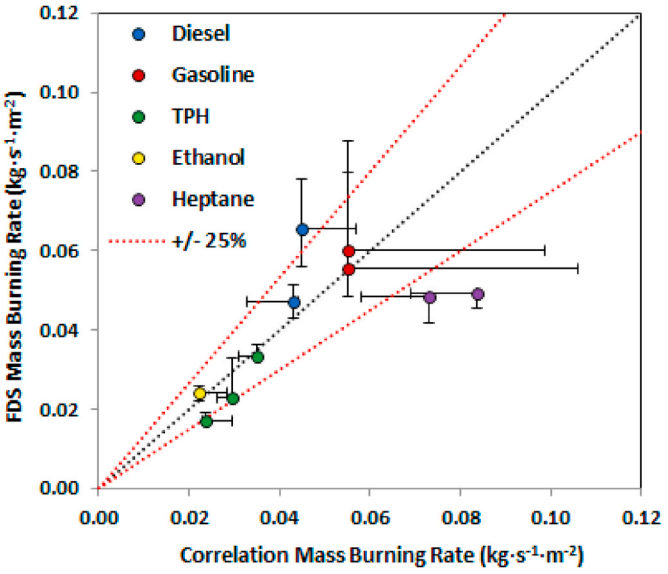

Fig. 9. Comparison of FDS-predicted quasi-steady mass burning rates to those estimated using the Babrauskas (1983) correlation. Vertical error bars show FDS grid sensitivity results. Horizontal error bars show the range of correlation estimates, including those using the Ditch et al. (2013) correlation, using the data in Table 4.

model than the experiment and the model predicts quasi-steady burning to occur much sooner than was observed. Using a smaller hot block as an ignition source could reduce the discrepancy between the observed and predicted fire growth. However, this method of ignition modelling is limited by the selected grid size in the model. Thus, it is clear that an alternative means of prescribing ignition for high boiling point liquid fuels in FDS is required to better represent ignition mechanisms used in experimental pool fire research.

The results shown here illustrate that including ignition modelling is likely to give a more representative initial rate of fire growth, delaying the onset of quasi-steady burning. However, another issue causing over-prediction of the growth rate is likely to be the use of infinite-rate combustion chemistry. As a consequence, there is no ignition delay in

the gas phase and the rate of fire growth and time taken to reach a quasi-steady burning regime are largely over-estimated in the model. A potential way forward would be to use a regime which combines infinite and finite-rate combustion chemistry. This would have the benefit of adding some control to the rate at which the combustion process progresses, enabling fuel to vaporise from the liquid fuel surface without undergoing combustion, at least initially. This would reduce the extent of heat feedback to the fuel surface in the early stages of the fire, lowering the fuel mass loss rate during the fire growth phase to give a more gradual period of fire growth, more comparable to that observed during the experiments.

4.2. Quasi-steady burning

Figs. 2 to 5 illustrate that the predicted quasi-steady burning rate generally compares well with the measurements across the range of fire scenarios considered. This result is consistent with previously published model comparison studies made using FDS (Hostikka et al., 2002; Rengel et al., 2018). However, it is also clear from these Figures that the quasi-steady burning regime is reached more quickly in the model than in the experiments and that the steady-state duration in the model exceeds that observed during the fire tests.

The original papers describing the experiments summarised in Table 3 give estimates of the timeframe during which the burning regime is considered to be quasi-steady. Averaging the burning rates predicted in the FDS simulations over the same timeframes allows direct comparison of predicted and measured steady-state burning rates for each scenario, as shown in Fig. 8. In this Figure vertical error bars have been included to show the level of mesh sensitivity across the FDS predictions. The dashed black line in the Figure indicates perfect agreement between the model and the measurements, with the two dashed red lines illustrating over and under prediction of the measured data by 25%. The Figure demonstrates that the FDS simulations performed here reproduce the measured quasi-steady burning rates to within 25% of the measurements for all tests except those involving gasoline as the fuel.

For the gasoline fire scenarios, the fuel was modelled using a single-component surrogate fuel with a single boiling temperature imposed, as described in Section 2.2.4. In reality, gasoline is a multi-component fuel comprising a range of hydrocarbons of different carbon chain lengths, each of which has a different boiling point. As a consequence, a gasoline pool fire would be expected to undergo preferential boiling of lower hydrocarbons before the heavier components burn off at a later stage of the fire, which is an effect that cannot be captured with the modelling approach adopted here. Predictions of gasoline pool fire burning rates could be improved by the inclusion of multi-component fuel effects and a range of boiling temperatures in the model. This would allow the burning rate to vary not only due to the incident heat flux at the fuel surface, but also as a result of different fuel components vaporising at a range of rates. In addition, the results show significant sensitivity to the choice of computational mesh for the gasoline fires, though the difference across meshes was reduced as the mesh resolution was increased.

Fig. 9 shows a similar comparison between the FDS-predicted quasi-steady burning rates and those estimated using the Babrauskas (1983) correlation. Again the vertical error bars indicate the level of FDS mesh sensitivity. In this Figure horizontal error bars show the variation in estimated steady burning rate across the Babrauskas (1983) and Ditch et al. (2013) correlations using the range of input parameter values given in Table 2. Fig. 8 illustrates that there is significant uncertainty in the steady-state burning rates estimated for both gasoline and heptane using the empirical correlations. This raises questions around the applicability of the input parameters listed in Table 2 for these two fuels. Comparison of burning rates estimated using the Babrauskas (1983) and Ditch et al. (2013) correlations to the measured data are presented in Section 4.4, which give a greater insight into the quantitative performance of these two models.

4.3. Fire extinction

A number of the fire scenarios considered here, namely the TPH fires of Pretrel at el. (2005) shown in Fig. 2 and the diesel fires of Chatris et al. (2001) and Muñoz et al. (2004) shown in Fig. 3, exhibit pre-extinction behaviours induced by complex physical mechanisms. Here, the pre-extinction phase can be considered the time period following quasi-steady burning, but before the true extinction process. For the TPH and diesel fires modelled in the present work, the time-varying burning rate curves exhibit a significant peak in burning rate during the pre-extinction period which is not captured in the FDS modelling. The physical mechanism responsible for causing such behaviour is fuel-dependent.

For the case of the diesel fires, the experimental configuration used a water sublayer beneath the fuel to stabilise the flame during the tests. During the latter stages of these fires, heat transferred through the fuel layer and into the water sublayer led to boilover and a significant increase in the measured burning rate. However, due to the measurement methods used, the experimental burning rate shown in Fig. 3 includes the cumulative mass of fuel and water vaporised during the boilover period, thus the difference between the model and measured data is smaller than it appears from the Figure.

For the TPH fires of Pretrel et al. (2005), no water sublayer was used and the increase in burning rate during the pre-extinction phase is a result of increased heat transfer between the fuel pan and the diminishing fuel layer. For these fire tests the influence of heat conduction becomes greater through the burn, leading to more vigorous vaporisation of fuel during the latter stages of the fire. From Fig. 2 it is clear that this is not captured in the FDS model results. This is likely due to the use of a one-dimensional heat conduction solution for the liquid fuel layer in the model. Incorporating two or three-dimensional heat conduction effects could lead to improved prediction of this phenomenon.

The liquid evaporation sub-model used in the FDS modelling presented here is based on a cell-by-cell solution method. A consequence of this is that the flame distribution over the fuel pan during the extinction phase of burning is not necessarily as expected. For the modelling described here, the results illustrate flame extinction beginning at the centre of the fuel pan before moving outwards to complete extinction at the fuel pan corners, as shown in Fig. 10 for the 0.4 m^2 TPH fire of Pretrel et al. (2005). The cell-by-cell solution procedure enables fuel to be consumed more quickly at the fuel pan centre than around the edges of the fuel pan due to the non-uniform distribution of heat feedback to the fuel surface. In reality, the remaining fuel would be able to flow within the fuel pan so as to remain at an approximately constant depth across the entire pan area until extinction. With the cell-by-cell solution method, FDS is not able to replicate this behaviour.

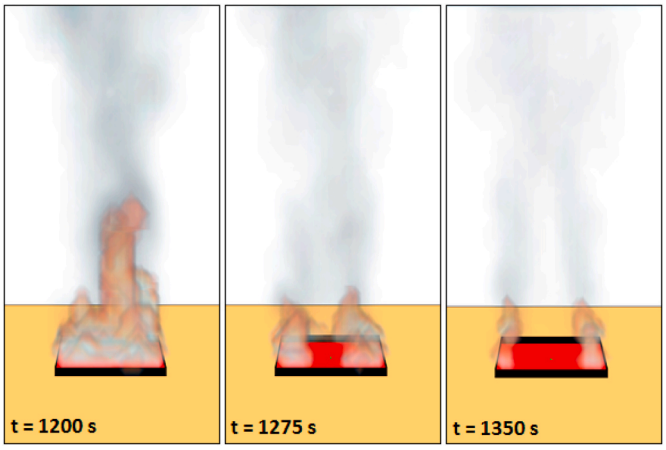

Fig. 10. FDS predicted extinction for the Pretrel et al. (2005) 0.4 m^2 TPH pool fire.

A further consequence of using a cell-by-cell solution for the fuel evaporation sub-model is that the model predicts a stepwise decay in burning rate during the extinction process, rather than a smoother transition from quasi-steady, or pre-extinction, burning to a state of extinction. Fig. 2 illustrates this behaviour most clearly for the FDS predictions of 0.4 m^2 TPH fire of Pretrel et al. (2005) during the period of 1000–1300 s after ignition. There is an inherent grid dependency associated with this behaviour, with the prominence of the step-wise decay in the transient burning rate profiles reduced as the grid resolution at the fuel surface is increased in the model. With an increase in grid resolution the transition of the flame from the pool centre to the pool edge is smoothed out, giving a clearer decay in burning rate through the flame extinction process.

In terms of the rate at which extinction occurs, the FDS results show reasonable agreement with the measured data for the majority of cases considered, as shown in Figs. 2 to 5. However, it is also clear from these Figures that the extinction process is often predicted to occur at a different time to that observed in the experiments. In the model, the time at which the extinction phase begins is governed by the fire behaviour preceding this phase of burning. Thus, for cases where FDS over-predicts the fire growth rate and the quasi-steady burning duration, such as for the Thomas et al. (2007) ethanol fire as shown in Fig. 4, the extinction phase occurs too soon in the model. This is a consequence of the fuel being consumed in the model more quickly than happens in the corresponding experiment, leading to prediction of early onset extinction. If predictions of pool fire growth could be improved, for example through the inclusion of finite-rate combustion chemistry, then it is likely that there would be improvements in the predicted extinction behaviour as a consequence.

4.4. Statistical Performance Measures

Fig. 11 shows *MG* plotted against *VG* for the transient fire quantities described in Section 2.3.1. Comparisons of FDS predictions to measured data are shown using circular symbols, comparison of empirical correlation estimates of quasi-steady burning rates to the measurements are shown as triangular symbols. The dashed black line in the Figure shows the line of no model bias and the dashed red lines show model bias within a factor of two. The solid black parabola shows the line of minimum variance. The dashed green lines indicate the region where $0.7 < MG < 1.3$ and $VG < 3.3$, which are the criteria suggested by Chang and Hanna (2004) to distinguish a 'good' atmospheric dispersion model. These criteria are included here for reference only, since they were not derived for fire models. The region enclosed by the green dashed lines in the Figure indicates model bias within ±30% of the mean with less than a factor of three scatter in model predictions.

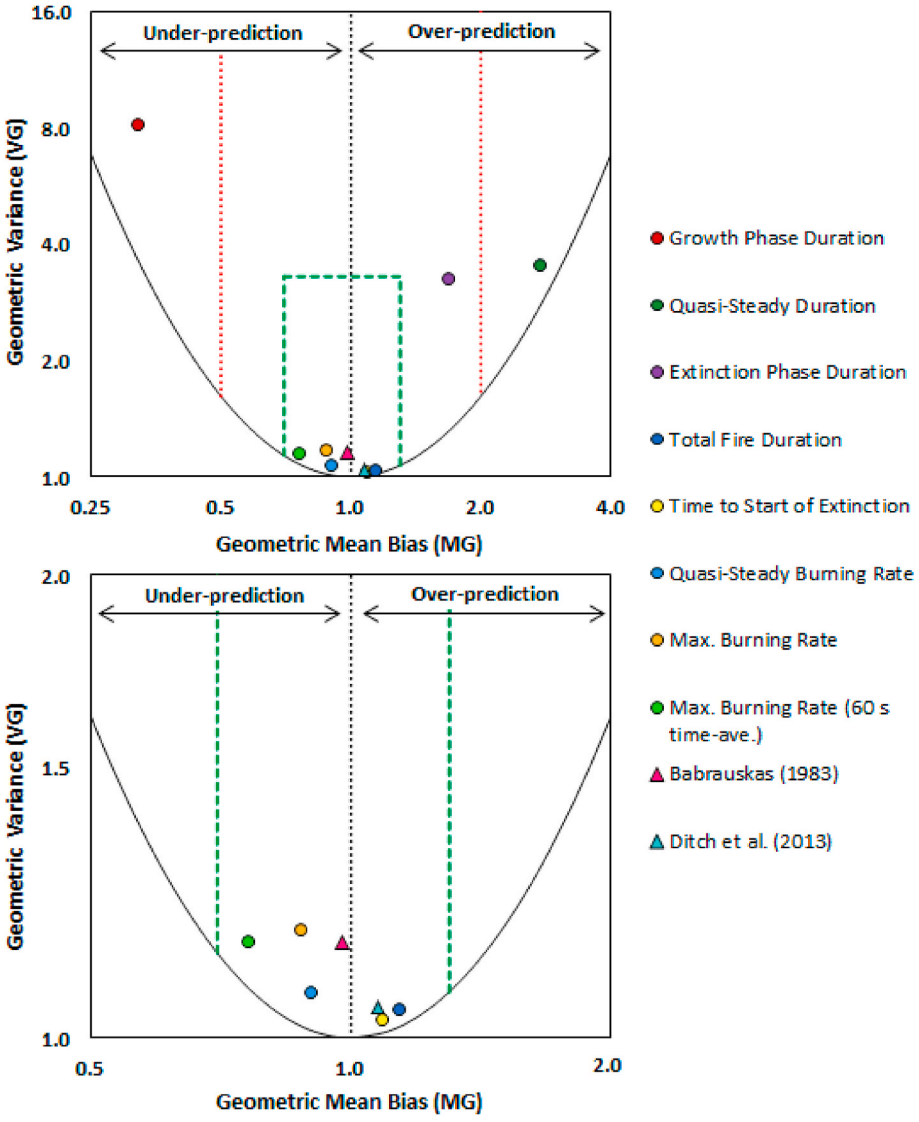

Fig. 11. Geometric mean bias (MG) against geometric variance (VG) for comparison of FDS predictions to experimental results (circles) and empirical correlations to measured data (triangles). Comparison of all data (top) and a close-up of a subset of the data (bottom) are shown for clarity. Lines of no model bias (dashed black), minimum model variance (solid black) and ± factor of two bias (dashed red) are also shown. The 'good' model criteria suggested by Chang and Hanna (2004), namely $0.7 < MG < 1.3$ and $VG < 3.3$, are included (dashed green) for reference. (For interpretation of the references to colour in this figure legend, the reader is referred to the Web version of this article.)

Fig. 11 demonstrates that the model significantly under-estimates the duration of the fire growth phase but predicts well, i.e. with little bias or scatter, the time at which the extinction phase begins and the total fire duration. Consequently, it follows that the model largely over-estimates the duration of the quasi-steady phase. Despite the model predicting the average time to the onset of the extinction phase and the total fire duration well, the duration of the extinction phase is over-predicted, on average, by almost a factor of two. Whilst this seems counterintuitive, it is a result of the SPM parameters analysing average model behaviour and in this case the value of *MG* is affected significantly by data from two tests, namely, the Muñoz et al. (2004) 1.5 m diesel fire and the 0.2 m^2 TPH fire of Pretrel et al. (2005). Referring back to Figs. 2 and 3 shows that for both of these tests the onset of the extinction phases is captured well by the model, but the duration of the burning rate decay is significantly over-predicted, resulting in a skewed value of *MG*. Removing these two tests from the calculation of *MG* for the extinction phase duration significantly decreases the model bias from $MG = 1.67$ to $MG = 1.14$, bringing the results within the bounds of the 'good' model criteria of Chang and Hanna (2004).

In terms of burning rates, Fig. 11 shows that the quasi-steady burning rate is slightly under-predicted by FDS on average, with very little scatter in the predictions, which indicates consistent model performance. Both the maximum burning rate and the maximum of the 60 s time-averaged burning rate are under-estimated by the model. Again, referring back to Figs. 2 to 5, it is clear that the under-predicted peak burning rates stem from a combination of the model under-predicting the burning rate for the two gasoline fires and as a result of the model failing to capture the behaviours observed during the pre-extinction phase for the TPH and diesels pool fires modelled. For the TPH fires, the peak burning rate is observed near extinction as a result of significantly increased heat conduction between the fuel and the fuel pan. For the diesel fires, the peak mass loss rates occur during a boilover phase prior to extinction. However, the methods used to measure mass loss rates in the experiments do not distinguish between vaporisation of fuel or water during the tests, thereby giving an unrealistically high measure of the peak burning rate. As such, the model does not under-predict the peak burning rate by as much as it would appear.

For a risk assessment or consequence modelling context, short-term effects of pool fires on their surroundings are most strongly related to the time at which the burning rate is maximized. Since the model has been shown to consistently under-predict the maximum burning rate, this raises questions about the use of the liquid pyrolysis modelling approach in FDS, in its present form, for predictive modelling in such contexts. To improve model predictions during the pre-extinction phase, the solution procedure could be modified to include two- or three-dimensional effects of heat conduction between the fuel pan and liquid fuel which, at present, are not accounted for in the model.

Fig. 11 also shows *MG* and *VG* for quasi-steady burning rates estimated using the correlations of Babrauskas (1983) and Ditch et al. (2013), compared to the measurements. The results show that the Babrauskas (1983) correlation gives good agreement with the data with practically no model bias. However, there is a reasonable amount of scatter in the predictions with $VG = 1.15$, equivalent to a factor of 1.5 scatter. The Ditch et al. (2013) correlation slightly over-estimates the quasi-steady burning rate ($MG = 1.07$), which is consistent with the results presented in Figs. 2 to 5, and does so consistently as demonstrated by the low variance across the results. For industrial applications, in which conservative estimates of fire consequences are preferable from a risk analysis perspective, the Ditch et al. (2013) correlation appears better suited than the correlation of Babrauskas (1983).

5. Conclusions

This work examined the ability of FDS to predict the transient burning rate of open atmosphere pool fires involving ethanol and a variety of liquid hydrocarbons as fuels for fires ranging from 0.4 m to 4 m in diameter and heat release rates of roughly 0.1 MW to 31 MW. Additional research would be required in order to characterise model performance for fire sizes greater than those simulated in the present study.

FDS consistently predicted a three phase transient burning rate profile which follows a consistent pattern of fire growth, quasi-steady burning and extinction. For the cases involving fuels with relatively low boiling temperatures (ethanol, heptane and gasoline) the default FDS combustion model resulted in instantaneous ignition and fire growth rates which greatly exceed those measured during the relevant experiments. Conversely, for the fuels with higher boiling temperatures, namely diesel and TPH, it was necessary to include a heat source in the model to initiate fuel ignition. For these fuels the initial rate of fire growth was predicted to be much slower, more closely matching the measured data. However, once the entire fuel pan surface was covered by the flame the fire growth rate again exceeded the rates observed in the relevant tests. It is clear that the use of infinitely fast combustion chemistry significantly over-predicts the rates of fire growth. Thus further work considering the impact of finite-rate, or a combination of infinite-rate and finite-rate reaction schemes would be a useful next step, as would evaluation of alternative ignition modelling approaches for high boiling temperature liquid fuels.

For all of the cases considered, the model predicted a long-duration quasi-steady period of burning. The predicted average steady-state burning rates were within 25% of the measurements for all but the two gasoline pool fires considered. In reality the multi-component nature of this fuel leads to preferential boiling of the fuel components having shorter-length hydrocarbon chains. This effect cannot be captured using a single surrogate fuel, as used in the present work. This is also relevant for modelling of diesel fires.

The duration of the predicted steady-state period consistently exceeded the measured quasi-steady duration. This was partly due to the model reaching the steady period of burning more quickly than in the experiments as a consequence of over-predicting the rate of fire growth. Additionally, failure of the model to capture the pre-extinction behaviour observed in some of the fire tests is a contributing factor.

The liquid vaporisation sub-model is based on a cell-by-cell solution procedure which results in fuel being consumed more quickly at the centre of the fuel pan than at the corners or edges. This is due to increased heat feedback to the fuel surface directly beneath the flame. Consequently, FDS predicted flame extinction to occur firstly at the pool centre before moving outwards to complete extinction at the corners of the fuel pan. This effect leads to a step-wise decay in burning rate in the FDS predictions, contrary to the smoothly decaying burning rate curves observed during the experiments. Despite this, the model provided a reasonable approximation of the overall rate at which extinction occurs.

Statistical analyses demonstrated that the bulk of the quantities of interest for transient liquid pool fire burning were predicted with relatively low model bias. In addition, the model predictions showed low levels of scatter, which demonstrated consistency across the results. The performance measures used in the analysis confirmed that FDS significantly over-estimated the rate of fire growth and the duration of the quasi-steady period of burning.

The maximum measured burning rates typically occurred during the pre-extinction phase of the burning process, however, this was not captured in the modelling. For the diesel fires, the observed peak burning rate resulted from the onset of thin-layer boilover. For the TPH fires, the peak burning rates resulted from increased conduction from the fuel pan to the diminishing fuel layer during the latter stages of burning. For the other fuels considered, peak burning rates were seen as fluctuations during quasi-steady burning. The FDS modelling showed consistent under-prediction of the peak burning rates. To improve model predictions during the pre-extinction phase, the solution procedure could be modified to include two- or three-dimensional effects of heat conduction between the fuel pan and liquid fuel.

The liquid pyrolysis sub-model in FDS gives consistent model

performance for fully predictive modelling of liquid pool fire burning rates. However, the model falls short of predicting the subtleties associated with the transient burning process. The results suggest a range of model modifications which could lead to improved prediction of transient fire growth and extinction for liquid pool fires. Specific topics for further research include: ignition modelling techniques more representative of those used experimentally; a combustion regime which combines infinite and finite-rate chemistry; a two- or three-dimensional heat conduction solution method for the liquid-phase; representing multi-component fuels, such as gasoline and diesel, using alternative surrogate fuels with ranges of boiling temperatures; alternative solution methods at the liquid-gas interface during fire extinction.

Declaration of competing interest

The authors declare that they have no known competing financial interests or personal relationships that could have appeared to influence the work reported in this paper.

Acknowledgements and Disclaimer

The authors would like to thank Mat Ivings, Graham Atkinson, Bronwen Ley, Richard Heaton and David Painter for their comments and feedback during preparation of this paper. This publication was funded by the Health and Safety Executive (HSE). The contents of the publication, including any opinions and/or conclusions expressed, are those of the authors alone and do not necessarily reflect HSE policy.

References

Abdolhamidzadeh, B., Abbasi, T., Rashtchian, D., Abbasi, S.A., 2011. Domino effect in process-industry accidents – an inventory of past events and identification of some patterns. J. Loss Prev. Process. Ind. 24, 575–593, 2011.

Aljumaiah, O., Andrews, G.E., Jimenez, A., Duhoon, N.R., Phylaktou, H.N., 2014. Fuel volatility effects on pool fires in compartments with low ventilation, *IAFSS, Fire Safety*. Science – Proceedings of the Eleventh International Symposium 331–345.

Audouin, L., Chandra, L., Consalvi, J.-L., Gorza, E., Hohm, V., Hostikka, S., Ito, T., Klein-Hessling, W., Lallemand, C., Magnusson, T., Noterman, N., Park, J.S., Peco, J., Rigollet, L., Suard, S., van Hees, P., 2011. Quantifying differences between computational results and measurements in the case of a large-scale well-confined fire scenario. Nucl. Eng. Des. 241, 18–31, 2011.

Babrauskas, V., 1983. Estimating large pool fire burning rates. Fire Technol. 19, 251–261.

Beji, T., Degroote, J., Merci, B., 2013. Parametric numerical analysis of fire-induced pressure variations in a well-confined and mechanically ventilated compartment. *Proceedings of the 6th European Combustion Meeting*.

Beji, T., Bonte, F., Merci, B., 2014. Numerical simulations of a mechanically-ventilated multi-compartment fire. IAFSS, Fire Safety Science – Proceedings of the Eleventh International Symposium 499–509.

Chamberlain, G.A., 1996. The hazards posed by large-scale pool fires in offshore platforms. Transactions of the IChemE 74, 81–87. Part B.

Chang, J.C., Hanna, S.R., 2004. Air quality model performance evaluation. Meteorol. Atmos. Phys. 87, 167–196, 2004.

Chang, J.I., Lin, C., 2006. A study of storage tank accidents. J. Loss Prev. Process. Ind. 19, 51–59, 2006.

Chatris, J.M., Quintela, J., Folch, J., Planas, E., Arnaldos, J., Casal, J., 2001a. Experimental study of burning rate in hydrocarbon pool fires. Combust. Flame 126, 1373–1383, 2001.

Chatris, J.M., Planas, E., Arnaldos, J., Casal, J., 2001b. Effects of thin-layer boilover on hydrocarbon pool fires. Combust. Sci. Technol. 171 (1), 141–161.

Darbra, R.M., Palacios, A., Casal, J., 2010. Domino effect in chemical accidents: main features and accident sequences. J. Hazard Mater. 183, 565–573, 2010.

de Ris, J., Orloff, L., 1972. A dimensionless correlation of pool burning data. Combust. Flame 18, 381–388.

Ditch, B.D., de Ris, J.L., Blanchat, T.K., Chaos, M., Bill Jr., R.G., Dorofeev, S.B., 2013. Pool fires – an empirical correlation. Combust. Flame 160, 2964–2974, 2013.

del Coro Fernández-Feal, M.M., Sánchez-Fernández, L.R., Sánchez-Fernández, B., 2017. Distillation: basic test in quality of automotive fuels. In: Mendes, M. (Ed.), *Distillation – Innovative Applications and Modeling*, IntechOpen. Accessed 27th July 2020, available from: https://www.intechopen.com/books/distillation-innovative-applications-and-modeling/distillation-basic-test-in-quality-control-of-automotive-fuels.

Hamins, A., Yang, J.C., Kashiwagi, T., 1999. A Global Model for Predicting the Burning Rates of Liquid Pool Fires, NISTIR 6381, National Institute of Standards and Technology, Gaithersburg, Maryland, USA, 1999.

Hanna, S.R., Chang, J.C., Strimatis, D.G., 1993. Hazardous gas model evaluation with field observations. Atmos. Environ. 27A (15), 2265–2285.

Hayasaka, H., 1997. Unsteady burning rates of small pool fires, IAFSS. Fire Safety Science – Proceedings of the Fifth International Symposium 499–510.

Hostikka, S., Kokkala, M.M.M., Vaari, J., 2001. Experimental Study of the Localized Room Fires – NFSC2 Test Series, VTT Research Notes 2104, VTT Technical Research Centre of Finland, Espoo, Finland, 2001.

Hostikka, S., McGrattan, K.B., Hamins, A., 2002. Numerical modeling of pool fires using LES and finite volume method for radiation. IAFSS, *Fire Safety Science – Proceedings of the Seventh International Symposium* 383–394.

Ivings, M.J., Gant, S.E., Jagger, S.F., Lea, C.J., Stewart, J.R., Webber, D.M., 2016. Evaluating Vapor Dispersion Models for Safety Analysis of LNG Facilities, second ed. Fire Protection Research Foundation (FPRF), National Fire Protection Association (NFPA), Quincy, MA, USA. Available from: https://www.nfpa.org/News-and-Research/Data-research-and-tools/Hazardous-Materials/LNG-model-evaluation-protocol-and-validation-database-update.

Le Saux, W., Pretrel, H., Lucchesi, C., Guillou, P., 2008. Experimental study of the fire mass loss rate in confined and mechanically ventilated multi-room scenarios. IAFSS, Fire Safety Science – Proceedings of the Ninth International Symposium 943–954.

Marsh, 2018. The 100 largest losses 1978-2017 – large property damage losses in the hydrocarbon industry. In: 25th Edition, Marsh & McLennan Companies, 2018.

Validation Guide McGrattan, K., Hostikka, S., McDermott, R., Floyd, J., Vanella, M., 2019a, 4th February 2019, available from:. In: sixth ed. Fire Dynamics Simulator Technical Reference Guide Mathematical Model. https://pages.nist.gov/fds-smv/manuals.html Verification Guide.

McGrattan, K., Hostikka, S., McDermott, R., Floyd, J., Vanella, M., 2019b. Fire Dynamics Simulator User's Guide, sixth ed., vol. 1019. NIST Special Publication. 4th February 2019, available from: https://pages.nist.gov/fds-smv/manuals.html.

MoPNG Committee, 2010. Constituted by Government of India) Independent Inquiry Committee Report on Indian Oil Terminal Fire at Jaipur on 29th October 2009, Completed 29th January 2010.

Muñoz, M., Arnaldos, J., Casal, J., Planas, E., 2004. Analysis of the geometric and radiative characteristics of hydrocarbon pool fires. Combust. Flame 139, 263–277, 2004.

Papanikolaou, E.A., Venetsanos, A.G., Heitsch, M., Baraldi, D., Huser, A., Pujol, J., Garcia, J., Markatos, N., 2010. HySafe SBEP-V20: numerical studies of release experiments inside a naturally ventilated residential garage. Int. J. Hydrogen Energy 35, 4747–4757, 2010.

Persson, H., Lönnermark, A., 2004. Tank Fires: Review of Fire Incidents 1951-2003, SP Report 2004:14, SP Technical Research Institute of Sweden, Borås, Sweden, 2004.

Prasad, K., Li, C., Kailasanath, K., Ndubizu, C., Ananth, R., Tatem, P.A., 1999. Numerical modelling of methanol liquid pool fires. Combust. Theor. Model. 3 (1999), 743–768.

Pretrel, H., Querre, P., Forestier, M., 2005. Experimental study of burning rate behaviour in confined and ventilated fire compartments. IAFSS, Fire Safety Science – Proceedings of the Eight International Symposium 1217–1228.

Pretrel, H., 2006. PRISME Source Program – Analysis Report, DPAM/SEREA-2005-015 – PRISME-2006-04 (Revision 1). IRSN, France.

Rengel, B., Christian, M., Elsa, P., Casal, J., Planas, E., 2018. A priori validation of CFD modelling of hydrocarbon pool fires. J. Loss Prev. Process. Ind. 56, 18–31, 2018.

SFPE, 2002. SFPE Handbook of Fire Protection Engineering, 3rd Edition, Society of Fire Protection Engineers, National Fire Protection Association, MA, U.S., 2002.

Sikanen, T., Hostikka, S., 2016. Modelling and simulation of liquid pool fires with in-depth radiation absorption and heat transfer. Fire Saf. J. 80, 95–109, 2016.

Sikanen, T., Hostikka, S., 2017. Predicting the heat release rates of liquid pool fires in mechanically ventilated compartments. Fire Saf. J. 91, 266–275, 2017.

Stewart, J.R., Kelsey, A., 2017. Numerical simulations of mechanically ventilated multi-compartment fires. In: Proceedings of SMiRT 24 15th International Seminar on Fire Safety in Nuclear Power Plants and Installations. Bruges, Belgium, p. 4, 5th October 2017.

Suard, S., Nasr, A., Melis, S., Garo, J., El-Rabii, H., Gay, L., Rigollet, L., Audouin, L., 2011. Analytical approach for predicting effects of vitiated air on the mass loss rate of large pool fire in confined compartments. IAFSS, *Fire Safety Science – Proceedings of the Tenth International Symposium* 1513–1524.

Suard, S., Forestier, M., Vaux, S., 2013. Toward predictive simulations of pool fires in mechanically ventilated compartments. Fire Saf. J. 2013 (61), 54–64.

Thomas, I.R., Moinuddin, K.A.M., Bennetts, I.D., 2007. The effect of fuel quantity and location on small enclosure fires. J. Fire Protect. Eng. 17, 85–101, 2007.

U.S. Nuclear Regulatory Commission, 2007. Office of Research/Electric Power Research Institute (EPRI): *Verification and Validation of Selected Fire Models for Nuclear Power Plant Applications, NUREG 1824*. U.S., Washington, DC vols. 1-7 May 2007.

van Hees, P., Wahlqvist, J., Hostikka, S., Sikanen, T., Husted, B., Magnusson, T., Jörud, F., 2014. Prediction and Validation of Pool Fire Development in Enclosures by Means of CFD Models for Risk Assessment of Nuclear Power Plants (Poolfire) – Final Report. Lund University, Sweden.

Vasanth, S., Tauseef, S.M., Abbasi, T., Abbasi, S.A., 2013. Assessment of four turbulence models in simulation of large-scale pool fires in the presence of wind using computational fluid dynamics (CFD). J. Loss Prev. Process. Ind. 26, 1071–1084, 2013.

Vipin, Pandey, S.K., Tauseef, S.M., Abbasi, T., Abbasi, S.A., 2018. Pool fires in chemical process industries: occurrence, mechanism, management. J. Fail. Anal. Prev. 18 (5), 1224–1261.

Wahlqvist, J., van Hees, P., 2013. Validation of FDS for large-scale well-confined mechanically-ventilated fire scenarios with emphasis on predicting ventilation system behaviour. Fire Saf. J. 62, 102–114, 2013.

Wahlqvist, J., van Hees, P., 2016. Implementation and validation of an environmental feedback pool fire model based on oxygen depletion and radiative feedback in FDS. Fire Saf. J. 85, 35–49, 2016.

Wen, J., Kang, K., Donchev, T., Karwatzki, J.M., 2007. Validation of FDS for the prediction of medium-scale pool fires. Fire Saf. J. 42, 127–138, 2007.
Yao, W., Yin, J., Hu, X., Wang, J., Zhang, H., 2013. Numerical modeling of liquid n-heptane pool fires based on heat feedback equilibrium. Procedia Engineering 62, 377–388, 2013.
Zadeh, S.E., Beji, T., Merci, 2015. Validation of the pyrolysis model of FDS 6 for a large-scale ethanol pool fire. In: Proceedings of the 9th Mediterranean Combustion Symposium, Rhodes, Greece, 7-11th June 2015.
Zadeh, S.E., Beji, T., Merci, B., 2016. Assessment of FDS 6 simulations results for a large-scale ethanol pool fire. Combust. Sci. Technol. 188 (4–5), 571–580.